

Supporting Information

Luminescent Nd₂S₃ thin films: A new chemical vapour deposition route towards rare-earth sulphides

Stefan Cwik^{a†}, Sebastian M. J. Beer^{a†}, Marcel Schmidt^b, Nils C. Gerhardt^c, Teresa de los Arcos^d, Detlef Rogalla^e, Jana Weßing^a, Ignacio Giner^d, Martin Hofmann^c, Guido Grundmeier^d, Andreas D. Wieck^b, Anjana Devi^{a*}

^a Inorganic Materials Chemistry, Ruhr University Bochum, 44801 Bochum, Germany

^b Applied Solid-State Physics, Ruhr University Bochum

^c Photonics and Terahertz Technology, Ruhr University Bochum

^d Macromolecular and Technical Chemistry, University Paderborn, 33098 Paderborn, Germany

^e RUBION, Ruhr University Bochum

† The author contributed equally to the paper.

Corresponding Author

*E-mail: anjana.devi@rub.de

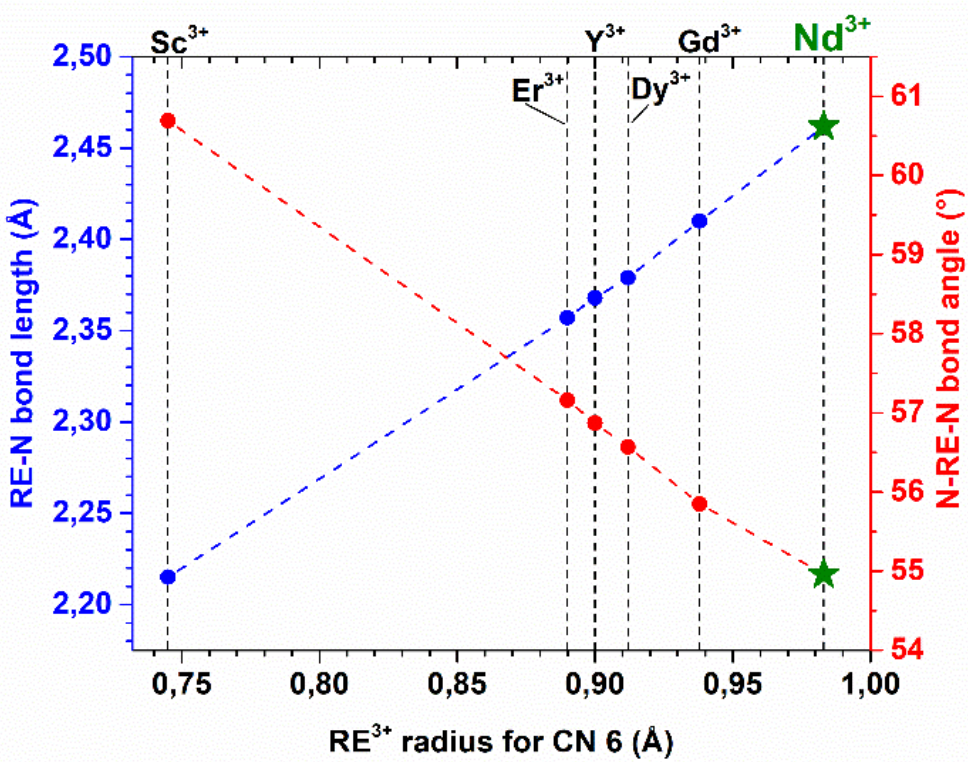


Figure S1: Relation and trend of RE^{3+} ionic radii to RE-N bond length (blue) and N-RE-N bond angle (red). The vertical black lines are guidance for the respective RE^{3+} ion. The graph was adapted and complemented from Milanov *et al* (A. P. Milanov, R. A. Fischer and A. Devi, Inorganic Chemistry, 2008, **47** (23), 11405).

Table S1: Selected structural parameters of **1** [Nd(dpdmg)_3] and published $[\text{RE(dpdmg)}_3]$. $\text{N}^{\text{a}} = -\text{N}^{\text{i}}\text{Pr}$, $\text{N}^{\text{b}} = -\text{NMe}_2$. Q1 and Q2 are centroid in the plane of $\text{N}_c\text{N}_d\text{N}_f$ and $\text{N}_x\text{N}_y\text{N}_z$ used to determine the mean torsion angle.

Compound	RE^{3+} radius (CN6) (Å)	Mean bond length (Å)		Mean bond angle (°)	Mean torsion angles (°)
		RE-N ^a	C-N ^b	N-RE-N	N-Q1-Q2-N
$[\text{Sc(dpdmg)}_3]$	0,745	2,215	1.398(4)	60,69	26.7
$[\text{Er(dpdmg)}_3]$	0,89	2,357	1.397(8)	57,16	20.5
$[\text{Y(dpdmg)}_3]$	0,9	2,368	1.396(8)	56,87	20.8
$[\text{Dy(dpdmg)}_3]$	0,912	2,379	1.397(4)	56,57	20.2
$[\text{Gd(dpdmg)}_3]$	0,938	2,41	1.396(8)	55,85	19.0
$[\text{Nd(dpdmg)}_3]\mathbf{1}$	0,983	2,4618	1.398	54,62	17.4

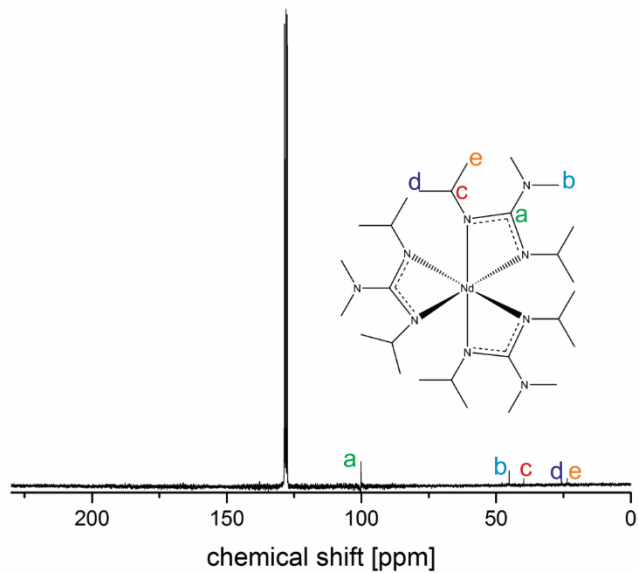


Figure S2: ^{13}C -NMR (200 MHz, C_6D_6) of $[\text{Nd}(\text{dpdmg})_3]$ **1**.

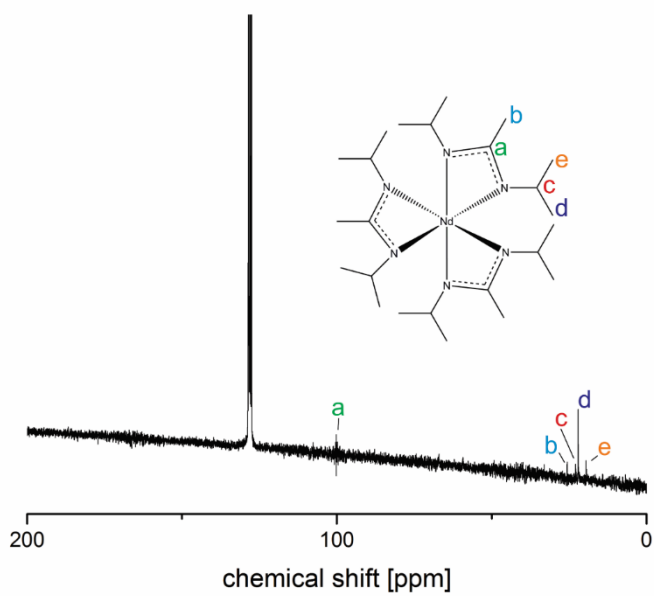


Figure S3: ^{13}C -NMR (200 MHz, C_6D_6) of $[\text{Nd}(\text{dpamd})_3]$ **2**.

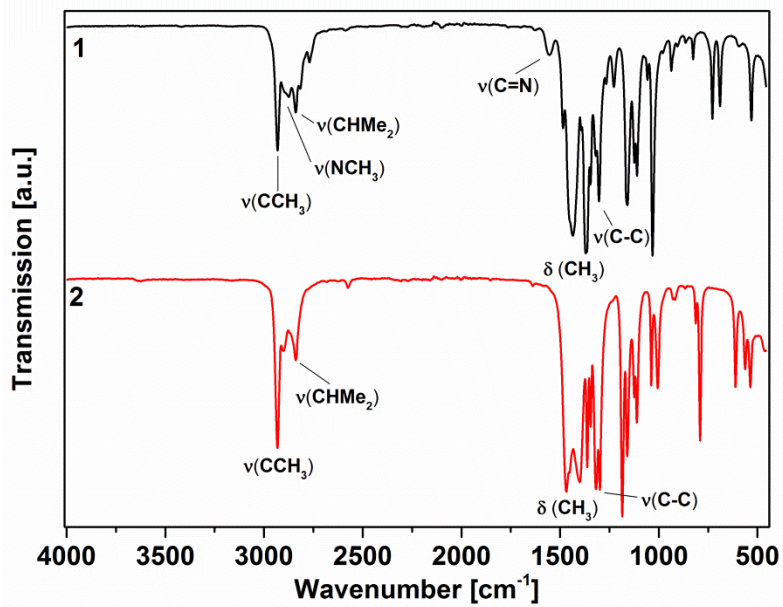
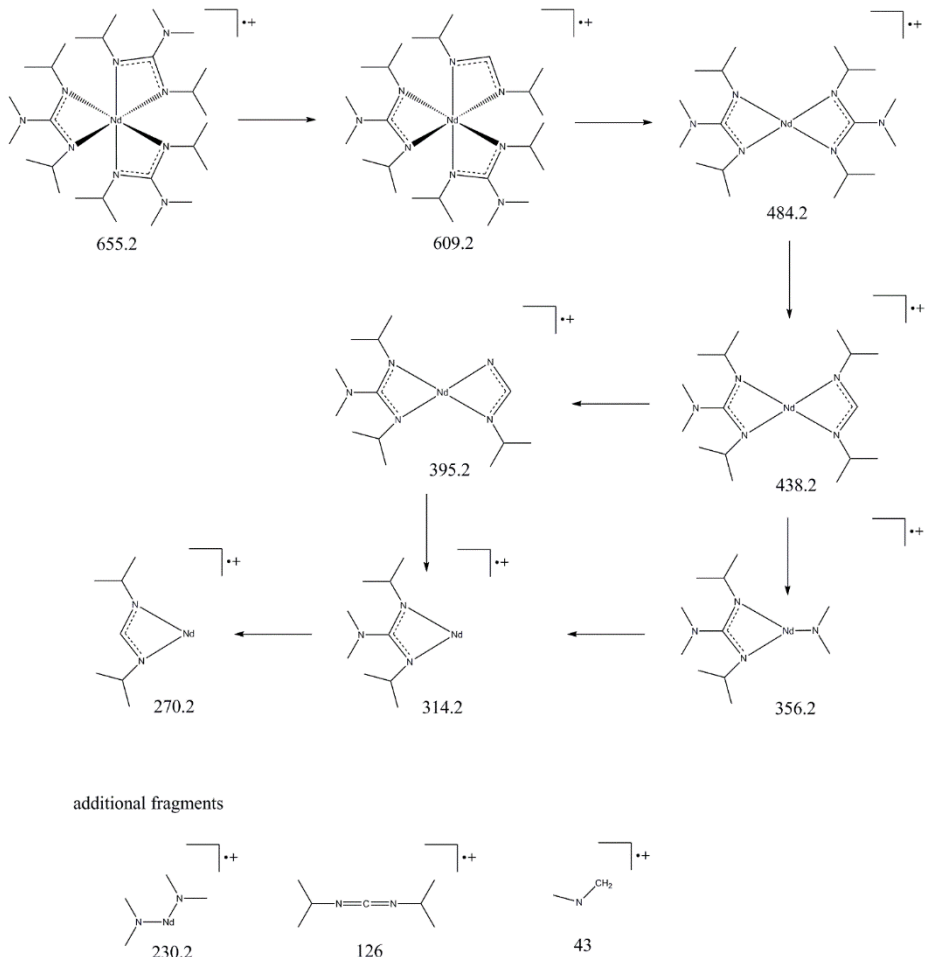


Figure S4: IR spectra of $[\text{Nd}(\text{dpdmg})_3]$ **1** (black) and $[\text{Nd}(\text{dpamd})_3]$ **2** (red).



Scheme S1: Proposed fragmentation pattern for $[\text{Nd}(\text{dpdmg})_3]$ 1.

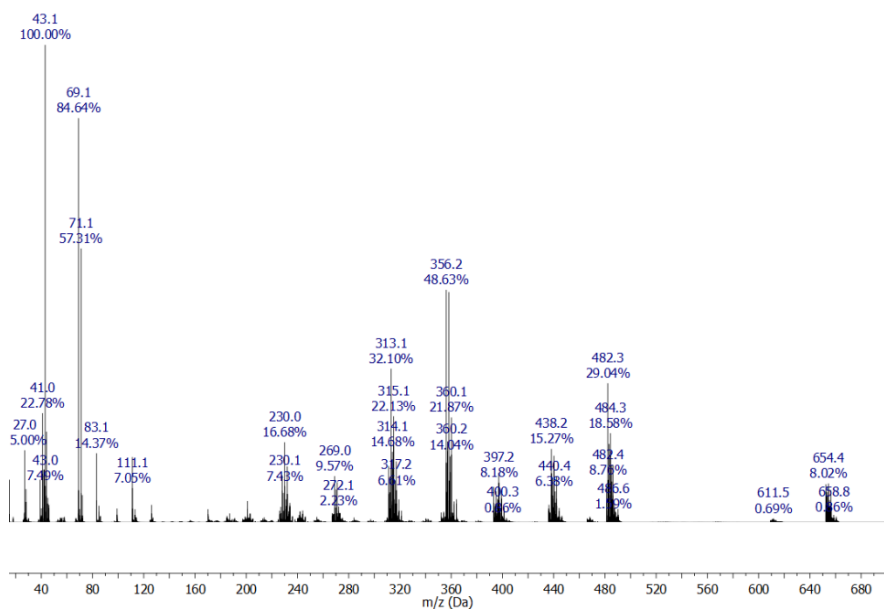
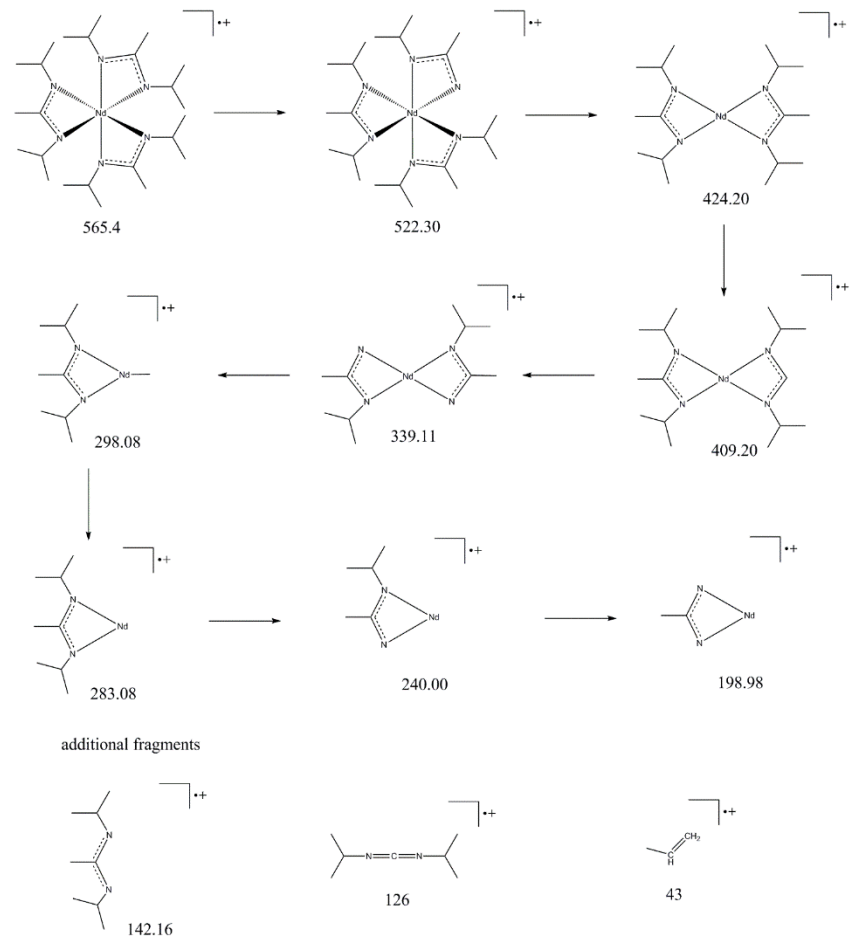


Figure S5: Mass spectrum of $[\text{Nd}(\text{dpdmg})_3]$ 1 (EI-MS, 70 eV).



Scheme S2: Proposed fragmentation pattern for $[\text{Nd}(\text{dpamd})_3]$ 2.

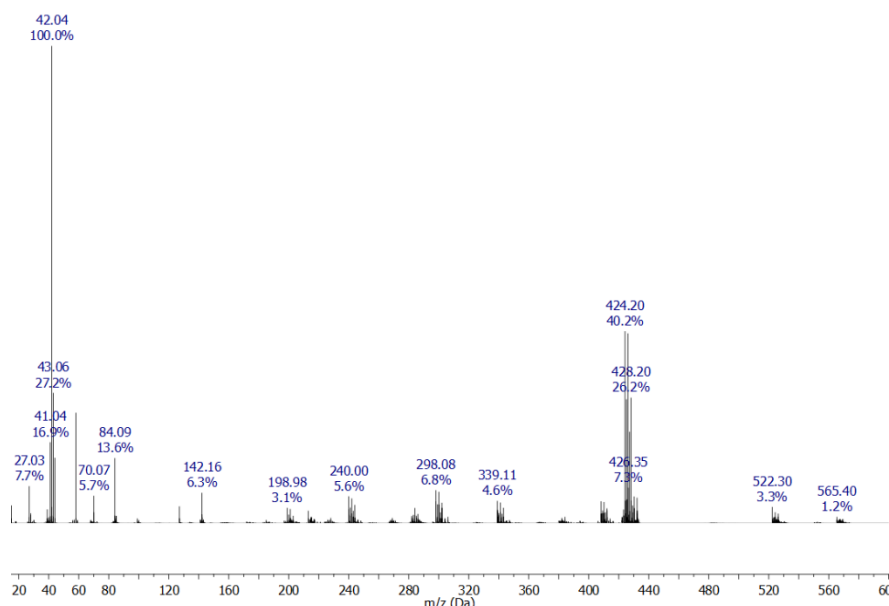


Figure S6: Mass spectrum of $[\text{Nd}(\text{dpamd})_3]$ 2 (EI-MS, 70 eV).

Table S2: Bond lengths for [Nd(dpdmg)₃] **1**.

Atom	Atom	Length/Å	Atom	Atom	Length/Å
Nd1	N1	2.448(2)	C10	N4	1.463(3)
Nd1	C13	2.901(2)	N9	C22	1.400(3)
Nd1	C22	2.896(2)	N9	C26	1.441(3)
Nd1	N8	2.450(2)	N9	C27	1.443(3)
Nd1	N7	2.487(2)	C9	N3	1.445(3)
Nd1	N5	2.455(2)	C22	N8	1.345(3)
Nd1	N4	2.474(2)	C22	N7	1.329(3)
Nd1	C4	2.913(2)	C23	C24	1.524(4)
Nd1	N2	2.494(2)	C23	C25	1.533(4)
C1	N1	1.466(3)	C23	N8	1.468(3)
C1	C3	1.520(4)	C21	C19	1.527(4)
C1	C2	1.513(3)	C20	C19	1.522(4)
N1	C4	1.342(3)	C19	N7	1.471(3)
C15	C14	1.531(3)	C8	N3	1.446(3)
C14	C16	1.525(3)	C7	C5	1.525(3)
C14	N5	1.470(3)	C18	N6	1.443(3)
C13	N6	1.395(3)	C17	N6	1.439(3)
C13	N5	1.331(3)	C6	C5	1.527(4)
C13	N4	1.349(3)	C5	N2	1.464(3)
C12	C10	1.525(4)	C4	N3	1.398(3)
C11	C10	1.527(4)	C4	N2	1.338(3)

Table S3: Bond angles for [Nd(dpdmg)₃] **1**.

Atom	Atom	Atom	Angle/ [°]	Atom	Atom	Atom	Angle/ [°]
N1	Nd1	C13	124.26(6)	N4	C13	N6	121.8(2)
N1	Nd1	C22	106.12(7)	C12	C10	C11	110.4(2)
N1	Nd1	N8	101.31(7)	N4	C10	C12	109.9(2)
N1	Nd1	N7	110.43(6)	N4	C10	C11	109.6(2)
N1	Nd1	N5	102.22(6)	C22	N9	C26	121.5(2)
N1	Nd1	N4	141.05(6)	C22	N9	C27	123.0(2)
N1	Nd1	C4	27.27(6)	C26	N9	C27	115.4(2)
N1	Nd1	N2	54.49(6)	N9	C22	Nd1	171.77(18)
C13	Nd1	C4	119.35(6)	N8	C22	Nd1	57.43(12)
C22	Nd1	C13	120.63(6)	N8	C22	N9	120.9(2)
C22	Nd1	C4	119.77(6)	N7	C22	Nd1	58.98(12)
N8	Nd1	C13	106.43(6)	N7	C22	N9	123.0(2)
N8	Nd1	C22	27.55(6)	N7	C22	N8	116.1(2)
N8	Nd1	N7	54.70(6)	C24	C23	C25	110.0(2)
N8	Nd1	N5	98.63(7)	N8	C23	C24	109.6(2)
N8	Nd1	N4	112.22(7)	N8	C23	C25	110.4(2)
N8	Nd1	C4	124.95(7)	C20	C19	C21	110.1(2)
N8	Nd1	N2	143.71(7)	N7	C19	C21	109.94(19)
N7	Nd1	C13	125.14(6)	N7	C19	C20	109.3(2)
N7	Nd1	C22	27.26(6)	C22	N8	Nd1	95.02(14)
N7	Nd1	C4	110.88(6)	C22	N8	C23	120.2(2)
N7	Nd1	N2	104.66(6)	C23	N8	Nd1	136.95(15)
N5	Nd1	C13	27.18(6)	C22	N7	Nd1	93.77(14)
N5	Nd1	C22	122.56(7)	C22	N7	C19	122.3(2)
N5	Nd1	N7	140.76(7)	C19	N7	Nd1	135.30(15)
N5	Nd1	N4	54.78(6)	C13	N6	C18	122.2(2)
N5	Nd1	C4	108.14(6)	C13	N6	C17	121.6(2)
N5	Nd1	N2	111.93(7)	C17	N6	C18	115.9(2)
N4	Nd1	C13	27.63(6)	C14	N5	Nd1	136.93(16)
N4	Nd1	C22	112.79(7)	C13	N5	Nd1	95.42(13)
N4	Nd1	N7	105.02(6)	C13	N5	C14	120.4(2)
N4	Nd1	C4	122.61(6)	C7	C5	C6	111.0(2)
N4	Nd1	N2	101.50(7)	N2	C5	C7	109.55(19)
N2	Nd1	C13	109.69(6)	N2	C5	C6	109.50(19)
N2	Nd1	C22	125.29(6)	C13	N4	Nd1	94.08(14)
N2	Nd1	C4	27.26(6)	C13	N4	C10	121.7(2)

N1	C1	C3	112.21(19)	C10	N4	Nd1	137.14(15)
N1	C1	C2	107.8(2)	N1	C4	Nd1	56.66(12)
C2	C1	C3	110.4(2)	N1	C4	N3	123.0(2)
C1	N1	Nd1	136.80(15)	N3	C4	Nd1	175.97(15)
C4	N1	Nd1	96.07(14)	N2	C4	Nd1	58.64(12)
C4	N1	C1	121.0(2)	N2	C4	N1	115.2(2)
C16	C14	C15	109.8(2)	N2	C4	N3	121.8(2)
N5	C14	C15	110.3(2)	C9	N3	C8	115.9(2)
N5	C14	C16	109.8(2)	C4	N3	C9	120.81(19)
N6	C13	Nd1	176.18(16)	C4	N3	C8	122.19(19)
N5	C13	Nd1	57.40(12)	C5	N2	Nd1	136.09(16)
N5	C13	N6	122.6(2)	C4	N2	Nd1	94.10(13)
N5	C13	N4	115.6(2)	C4	N2	C5	121.25(19)
N4	C13	Nd1	58.29(12)				

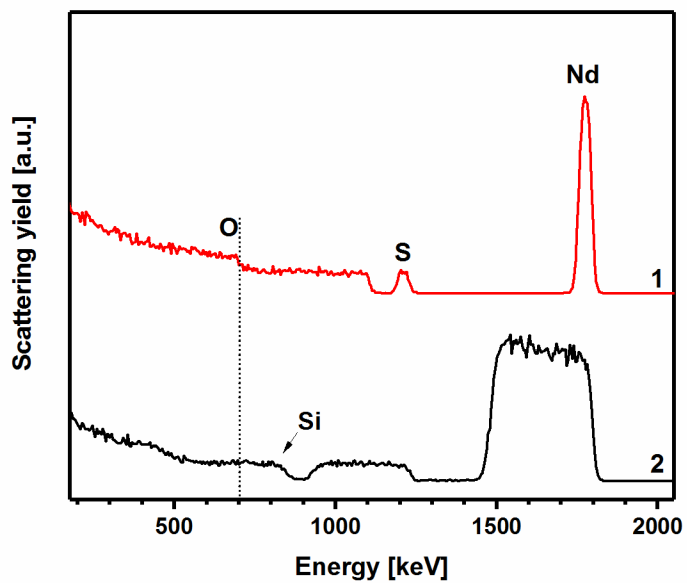


Figure S7: RBS spectra Nd_2S_3 thin films deposited using $[Nd(dpdmg)_3]$ **1** and $[Nd(dpamd)_3]$ **2** on fused silica at 500 °C.

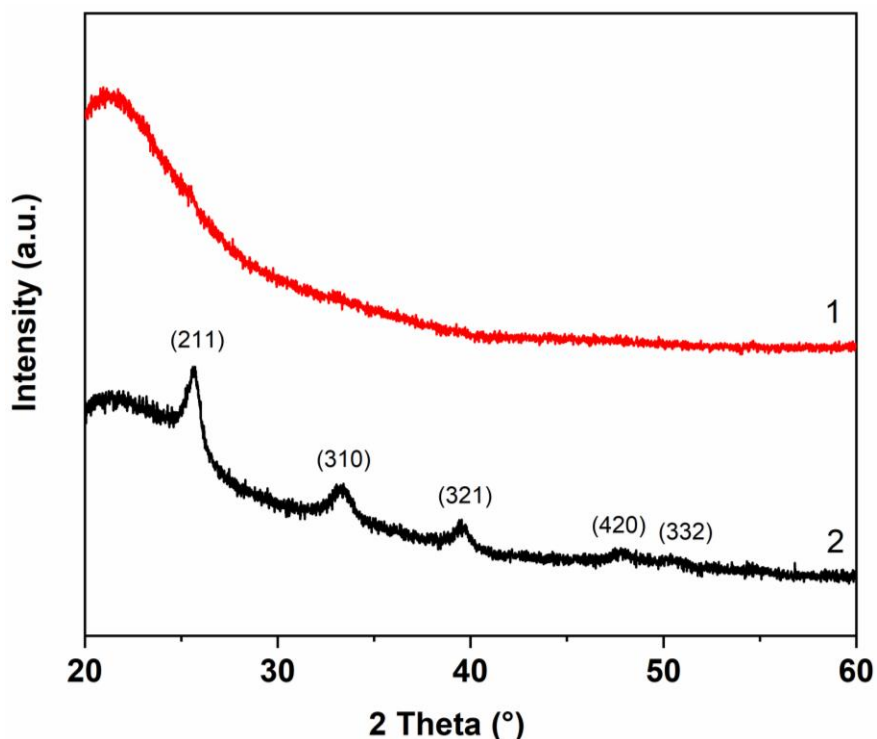


Figure S8: XRD patterns of Nd_2S_3 thin films on fused silica grown from $[\text{Nd(dpdmg)}_3]$ **1** and $[\text{Nd(dpamd)}_3]$ **2** at 500 °C. All indices correspond to the cubic (I-43d) Nd_2S_3 reference ICSD 64582063. The XRD data was not background corrected.

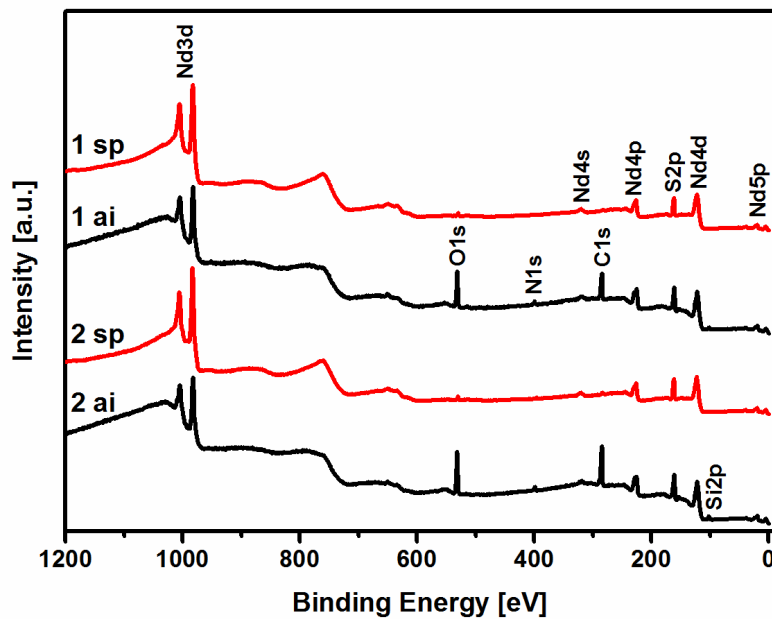


Figure S9: XPS survey spectra Nd_2S_3 thin films deposited from $[\text{Nd(dpdmg)}_3]$ **1** and $[\text{Nd(dpamd)}_3]$ **2** on Si(100) at 500 °C before (ai) and after sputtering (sp).

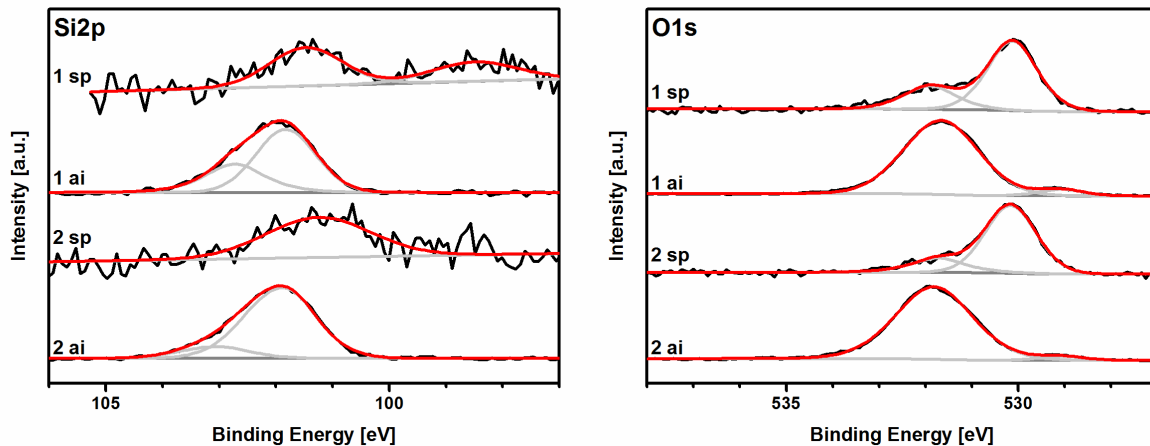


Figure S10: Normalized Si 2p and O 1s core-spectra of Nd₂S₃ thin films deposited from [Nd(dpdmg)₃] **1** and [Nd(dpamd)₃] **2** deposited at 500 °C before (ai) and after sputtering (sp).

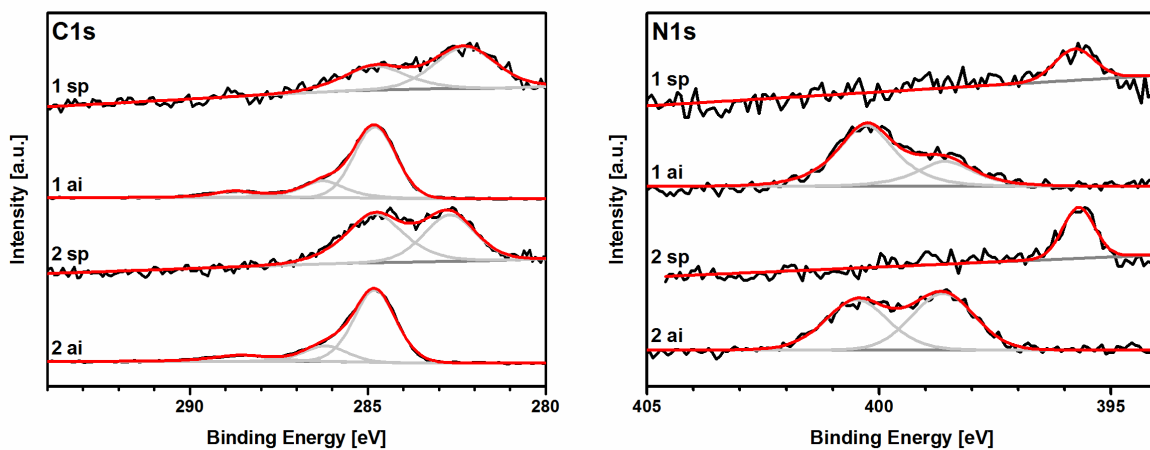


Figure S11: Normalized C1s and N1s core-spectra of Nd₂S₃ thin films deposited from [Nd(dpdmg)₃] **1** and [Nd(dpamd)₃] **2** deposited at 500 °C before (ai) and after sputtering (sp).

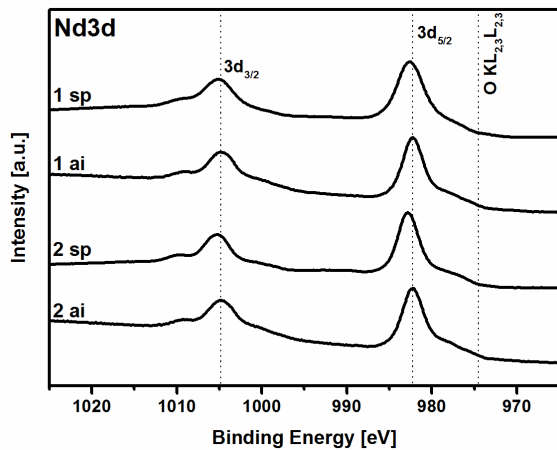


Figure S12: Normalized Nd3d core-spectra of Nd_2S_3 thin films deposited from $[\text{Nd}(\text{dpdmg})_3]$ **1** and $[\text{Nd}(\text{dpamd})_3]$ **2** deposited at 500 °C before (ai) and after sputtering (sp).

Nd3d: The maximum of the $3d_{5/2}$ peak (see Fig. S12) shifts from 982.2 to 982.7 eV after sputtering and the $3d_{3/2}$ peak maximum appears at a higher binding energy (0.4 eV) in the bulk with respect to the film surface (1004.8 eV). The peak positions after sputtering are in agreement with the values reported Nd_2S_3 quantum dots¹. The low energy shift before sputtering can be explained by the higher contribution of metallic Nd to the core-level spectra which occur at around 980 eV^{95–103}.

Table S4: Binding energies (BE) of the employed fit functions and their contribution to the thin film composition on the surface (ai) and in the bulk (sp) of the Nd₂S₃ thin films deposited from [Nd(dpdmg)₃] **1** and [Nd(dpamd)₃] **2**. Elemental composition was determined with CASA XPS software, the contribution of the fit functions to each element was obtained with Unifit.

Peak	1 ai		1 sp		2 ai		2 sp	
	BE (eV)	at. %						
<i>C1s</i>	284.8	26.60	282.3	0.78	284.8	30.76	282.7	4.61
	286.3	7.39	284.8	0.49	286.2	6.93	284.8	5.71
	288.8	2.78			288.6	3.78		
<i>N1s</i>	398.6	0.27	395.8	0.13	398.6	2.07	395.7	2.00
	400.3	0.67			400.5	1.85		
<i>O1s</i>	529.1	0.93	530.1	1.01	529.1	0.54	530.2	3.46
	531.7	16.92	531.9	0.37	531.8	15.79	531.7	0.88
<i>Si2p</i>	101.8	1.69	98.5	0.08	101.7	3.75	101.3	0.73
	102.7	0.83	101.5	0.13	102.9	0.63		
<i>S2p</i>	160.5	11.91			160.4	9.21		
	161.4	10.04	161.5	40.15	161.4	9.46	161.2	37.75
	163.4	2.21	163.0	8.25	163.6	3.39	162.1	10.95
	167.0	1.04			167.0	0.15		
<i>Nd4d</i>	115.3	0.82	116.2	3.05	116.3	1.37	115.4	1.84
	118.8	6.14	119.1	12.83	118.7	3.78	118.9	12.10
	121.6	7.35	121.9	20.93	121.3	6.54	121.8	19.97

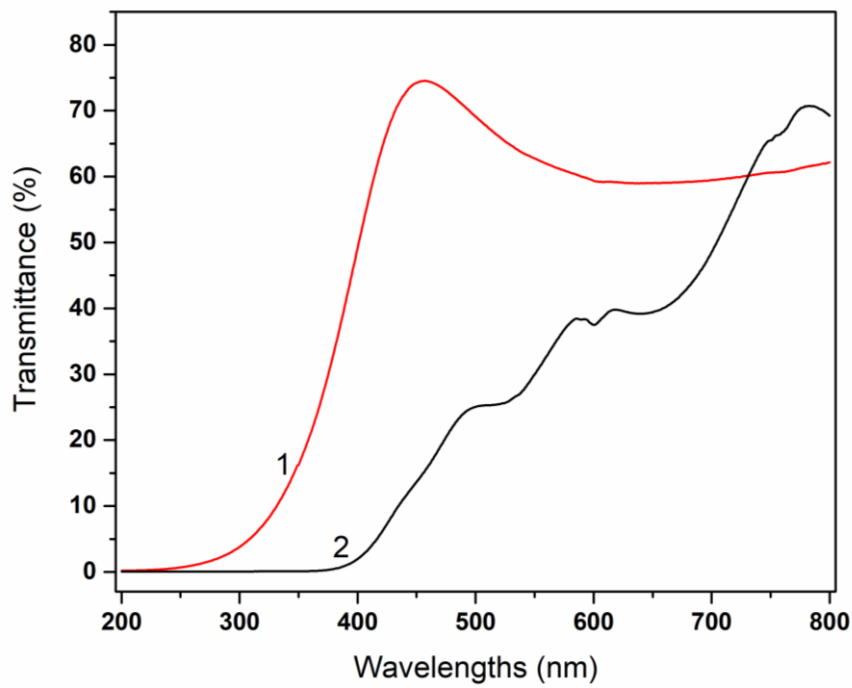


Figure S13: UV-Vis transmission spectrum of Nd_2S_3 thin films grown at 500 °C on fused silica from $[\text{Nd}(\text{dpdmg})_3]$ **1** and $[\text{Nd}(\text{dpamd})_3]$ **2**.

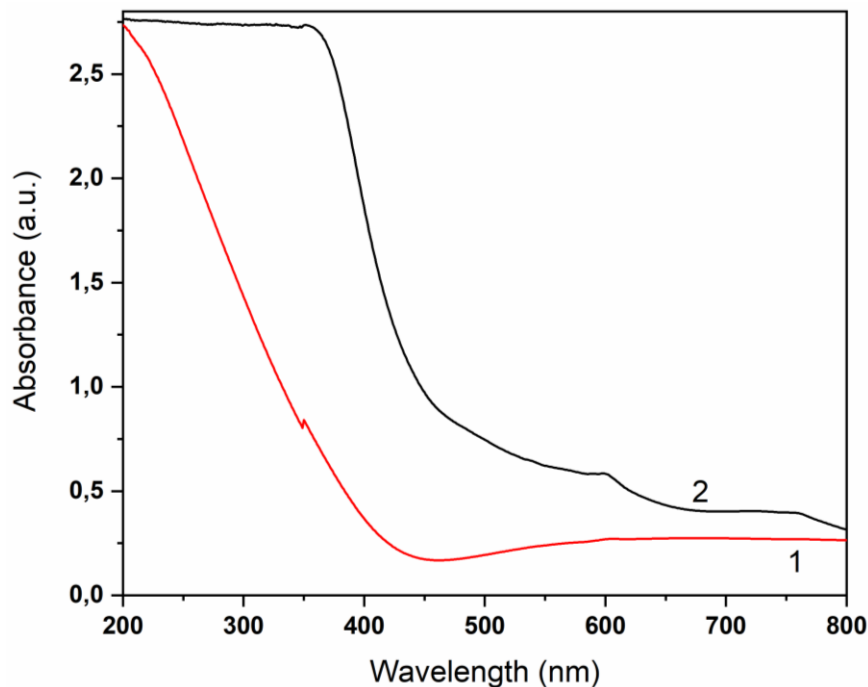


Figure S14: UV-Vis absorption spectrum of Nd_2S_3 thin films grown at 500 °C on fused silica from $[\text{Nd}(\text{dpdmg})_3]$ **1** and $[\text{Nd}(\text{dpamd})_3]$ **2**. The small offsets at around 350 nm occurs due to the change of the radiation sources during the measurements.